C.P. No. 1190

C.P. No. 1190

MINISTRY OF DEFENCE (PROCUREMENT EXECUTIVE)

AERONAUTICAL RESEARCH COUNCIL

CURRENT PAPERS

An Experimental Investigation of Supersonic Boundary-Layer Flows with Pressure Gradients

By

S. Sivasegaram
Department of Mechanical Engineering,
Imperial College

LONDON. HER MAJESTY'S STATIONERY OFFICE

1971

Price 56p net

C.P. No.1190*
July, 1969

An Experimental Investigation of Supersonic Boundary-Layer Flows with Pressure Gradients

- By -
S. Sivasegaram
Department of Mechanical Engineering,
Imperial College

SUMMARY

The report presents measurements made in the small supersonic wind tunnel at the National Physical Laboratory, Teddington. Boundary layer measurements in two favourable and one adverse pressure gradient are analysed. The report also includes a more detailed study of some zero pressure gradient measurements, made with the same apparatus and reported earlier, and a study of the performance of the floating element skin friction balance in pressure gradients.

Contents/

---

* Replaces A.R.C.31 586

Contents

List/

List of Figures

Nomenclature/

Nomenclature

Symbol	Meaning	Definition
A	Constant in the law of the wall	
C	" " " " " " "	
c_f	Skin friction coefficient	$2\,\tau_\omega/\rho_G u_G^2$
D	Diameter of floating element	
M	Mach number	
M_τ	Friction Mach number	$(\tau_\omega/\gamma p)^{\frac{1}{2}}$
p	Static pressure	
p_{stag}	Settling chamber stagnation pressure	
p_{tot}	Total (or pitot) pressure	
r	Recovery factor	
R	Reynolds number	
T_G	Mainstream static temperature	
T_{stag}	Settling chamber stagnation temperature	
T_{wall}	Temperature of floor of working section	
u	Velocity in x direction	
u_τ	Friction velocity	$(\tau_\omega/\rho_\omega)^{\frac{1}{2}}$
u^+		$\frac{u_G}{u_\tau}\left(\frac{1}{\alpha}\sin^{-1}\left(\alpha\frac{u}{u_G}\right)\right)$
v	Velocity in y direction	
x	Distance from first throat along flow direction	
y	Distance normal to floor	
α		$\left(\frac{\gamma-1}{2}\cdot\frac{r\,M_G^2}{1+\frac{\gamma-1}{2}r\,M_G^2}\right)^{\frac{1}{2}}$
γ	Ratio of specific heats	

δ_1 /

Nomenclature (contd)

Symbol	Meaning	Definition
δ_1	Boundary layer displacement thickness	$\int_0^\infty \left(1 - \frac{\rho u}{\rho_G u_G}\right) dy$
δ_2	Boundary layers momentum thickness	$\int_0^\infty \frac{\rho u}{\rho_G u_G}\left(1 - \frac{u}{u_G}\right) dy$
$\delta_{.99}$	Value of y where $u = 0{\cdot}99\ u_G$	
K	Mixing length constant in wall region	
μ	Dynamic viscosity (laminar)	
ν	Kinematic viscosity	μ/ρ
ρ	Density	
τ	Shear stress in x direction, parallel to floor	

Subscripts

G	Main stream
ω	Floor of working section
x	Properties evaluated with reference to x
1	" " " " " δ_1
2	" " " " " δ_2

1./

1. Introduction

In a previous report[1] B. Edwards and the present author presented measurements carried out in the boundary layer of a zero pressure gradient flow at a nominal Mach number of 2·2. The present report is concerned with similar measurements carried out in the same wind tunnel but in the presence of longitudinal pressure gradients. The influence of adverse and favourable pressure gradients on the hydrodynamic properties of the boundary layer is demonstrated. The severity of the pressure gradient is exemplified (a) by the Mach number range which was 2·7 to 2·1 for the adverse pressure gradient and 1·8 to 2·4 for the favourable pressure gradients, all achieved over a distance of approximately 2 feet, and (b) by the parameter $[(\delta_1/\tau_\omega).\ dp/dx]$ (= the ratio between the pressure gradient and skin friction terms in the integral momentum equation) which is of the order 0·35 for the adverse pressure gradient and -0·25 for the favourable pressure gradients.

The main purpose of the present report is to present the results of the experimental programme in a form suitable for comparison with results of prediction procedures. The implications of the results and the likely experimental precision are discussed and further comments on the earlier results of Ref. 1 are included. The sections on the apparatus, experimental procedure and precision are detailed only in so far as they refer to non-zero pressure gradient situations: a more detailed account of these items, for zero pressure gradient situations, may be found in Ref. 1. A lay-out diagram of the wind tunnel is shown in Fig. 1. The air, which is supplied from a high pressure storage system, flows through quick action and gate valves before entering the working section through a settling chamber; it leaves through a subsonic diffuser placed downstream of the second, and adjustable, throat. The rectangular working section has a constant width of 1 foot and is constructed in two parts. The upstream section has a flexible steel roof and a rigid gun-metal floor; the downstream section has a rigid, adjustable, gun-metal roof and a gun-metal floor. The side walls of the working section are of steel throughout.

2. Apparatus

No apparatus changes were necessary to achieve the favourable pressure gradients presented here. The flexible upstream section of the roof and the inflexible downstream section of the roof were adjusted to give the strongest possible favourable pressure gradient compatible with the equipment and the requirement that the longitudinal static pressure distribution should have no discontinuities. In the case of the adverse pressure gradient, however, an apparatus change was necessary. In this case the arrangement of the roof to give the strongest possible adverse pressure gradient compatible with the equipment implied that a normal shock wave remained just downstream of the first throat and, consequently, that the downstream flow was subsonic. In order to overcome this defect, the downstream section of the roof was hinged at its leading edge; this allowed it to swing by approximately 10°. Thus, on starting, the build-up in static pressure inside the nozzle lifted the downstream portion of the roof to its highest position and enabled the wind tunnel to start; once started, the static pressure fell and the hinged roof returned to its lowest position and the flow to the required adverse pressure gradient. Two pairs of single-acting dashpots were provided to damp the motion of the roof in both directions.

For/

For each of the three pressure gradients presented here boundary layer trips were provided in the region of the first throat. For the first favourable pressure gradient, a Sellotape trip was used; for the adverse pressure gradient, a half inch strip of 200/230 carborundum powder was glued to the floor; and for the second favourable pressure gradient, a one inch strip of 200/230 carborundum was glued to the floor.

The instrumentation was identical to that used in Ref. 1. In addition to a flattened total pressure probe (0.045 inch x 0.006 inch internal dimensions and 0.040 inch x 0.002 inch internal dimensions), measurements were carried out with a round total pressure probe of dimensions 0.012 inch o.d. and 0.004 inch i.d.

A novel design of surface tube was used for skin friction measurements. Two slots, each 0.16 inch long by 0.004 inch wide were made on a diameter of a $\frac{1}{2}$ inch rod whose end was flush with a standard floor plug. A ramp depression of 0.0015 inch maximum depth and 0.20 inch long was made ahead of one slot creating in effect a step on the plug surface. The slots were connected via metal and flexible tubing to the limbs of a U-tube water manometer. The pressure difference that the manometer recorded was that between the static and essentially total pressures immediately adjacent to the plug surface.

The surface tube was calibrated in zero pressure gradient against a floating element balance (Ref. 1) to obtain a relationship between the pressure difference reading and the skin friction. Periodic checks of the low speed calibration were made in a square pipe.

3. Experimental Procedure and Results

3.1 Arrangement of the longitudinal pressure distributions

In order to achieve the requirements of the strongest possible pressure gradient and an absence of discontinuities in the static pressure distribution, the roof of the working section was initially set on the basis of one-dimensional isentropic flow theory with allowance for the boundary-layer displacement thickness. The static pressure distribution along the floor centre line was then measured and the roof setting adjusted until a satisfactory distribution was obtained. The three static pressure distributions used for the present investigation are shown in Fig. 2, and the corresponding Mach number distributions are shown in Fig. 3.

The static pressure distribution for the first favourable pressure gradient can be represented by a smooth curve from which, between ports 1 and 11, the maximum deviation of an experimental point is 3%. The Mach number range between these ports is 1.8 to 2.4. The static pressure distribution for the adverse pressure gradient also showed a maximum deviation of 3% from a smooth curve up to port 11: but in this case, the adverse pressure gradient began at port 4; between ports 4 and 11 the Mach number range was 2.7 to 2.15. The maximum deviation of static pressure measurements from a smooth curve in the case of the second favourable pressure gradient was 3% between ports 1 and 10 and the Mach number range was 1.8 to 2.45.

3.2 Experimental checks

The two-dimensionality of the flow and the repeatability of the measurements were tested for all pressure gradients in the manner described in detail in Ref. 1. Flow visualisation using oil; static pressure measurements $\frac{3}{4}$" to either side of the centre line of the floor of the working section; and

Preston tube measurements over the centre 10 inches of the working section revealed no significant deviations from two-dimensionality. Measurements of total pressure in the working section revealed no significant change over the period of time required to complete a run; repetition of some velocity profile and skin friction measurements showed no significant difference in the results.

3.3 Velocity profile and skin-friction measurements

Total pressure profiles were measured at ports 1 to 11 for the first pressure distribution using the flattened total pressure probe. The resulting velocity profiles are shown in Fig. 7 in compressible law of the wall co-ordinates, (see Section 5.5). The corresponding velocity profiles for the adverse pressure gradient and the second favourable pressure gradient are shown in Fig. 8 and 9*, respectively, and are discussed in detail in Section 5.

It may be seen from Fig. 7 that the boundary layer was not fully turbulent upstream of port 4. A similar situation is revealed by Fig. 8, although a carborundum boundary layer trip was used. The results in Fig. 9 indicate a fully turbulent boundary layer from port 1; in this case a longer carborundum trip was employed. The values of momentum thickness and skin friction coefficient corresponding to the measurements shown in Figs. 7 to 9 are shown on Figs. 4 and 5; the values of momentum thickness were obtained in a manner similar to that described in Ref. 1 but with allowance for the variation of static pressure normal to the floor (see Section 4) and the values of skin friction using the calibrated surface probe. The subsonic calibration of the surface probe was repeated after each pressure gradient to determine if erosion had altered the probe characteristics; differences in calibration implying an increase of at most 2% in the calculated values of skin friction, were discovered and considered insignificant.

The floating element balance, previously described in Ref. 1 and used in zero pressure gradients, was tested in the first favourable and adverse pressure gradients. The results are shown in Fig. 15 in the form of an error plot.

4. Experimental Precision

A detailed discussion of experimental precision in zero pressure gradient situations was presented in Ref. 1. The experience gained in the present series of experiments has suggested some minor changes to the estimates of precision; these are shown in Table 1 and discussed below.

The error assessments of Ref. 1 did not include the possible effect of non-uniformity of the static pressure distribution. This could give rise to errors up to 0.5% in u/u_G.

A significant source of error in the evaluation of momentum thickness was overlooked in Ref. 1; this concerns the uncertainty in determining the outer edge of the boundary layer. This is especially significant for the velocity profiles measured in regions having a strong local pressure gradient, since the total pressure tube reading in the free stream of a supersonic flow is a function of local Mach number. The static pressure normal to the floor is not constant for a supersonic flow with pressure gradient and, consequently, it is not possible to accurately estimate the edge of the boundary layer on the basis of total pressure tube readings. The ambiguities caused by this factor have been eliminated in the present work by taking into account the variation of static pressure normal to the floor in the calculation of velocity profiles. Fig. 12 clearly demonstrates the difference in the Mach number profiles obtained with and without the allowance for variation of static pressure normal to the floor in favourable and adverse pressure

gradients/

* Tabulated data is available on request.

gradients. The difference between the static pressure at the wall and at the edge of the boundary layer in the case of a typical profile is of the order 2 to 3% although it is of the order 10% in the region of port 1 for all the reported pressure gradients. The maximum differences in u/u_G and δ_2 calculated by the present procedure and that used in Ref. 1 are 2% and 5%, respectively; the average differences are approximately 1% and 2%. This leads to an additional uncertainty of the order 2% in δ_2.

The possibility of total pressure tube errors due to "displacement effects" was explored by repeating two of the velocity profile measurements in the second pressure gradient with the round total pressure tube. The differences were well within the estimated experimental error (0.0005 to 0.001 in y) and hence errors due to "displacement effects" were considered negligible.

Table 1

Summary of overall errors

Item	Maximum error	Reproducibility
p_{stag}	±0.5%	-
p	"	-
p_{tot}	"	-
u/u_G	±1.5%	1%
δ_2	±3%	2%
τ_ω (surface probe)	±1%	2%
τ_ω (floating element balance)	±3.5%	2%

5. Discussion of Results

The present measurements are discussed in the sequence in which they have been obtained. This is followed by a discussion of the zero pressure gradient measurements reported in Ref. 1 and of the implications of the present results, and those of Ref. 1, on the law of the wall; finally, the results of the floating element balance are discussed.

5.1 The first favourable pressure gradients

The variation of the parameter $[(\delta_1/\tau_\omega).dp/dx]$ with distance is shown on Fig. 14. $[(\delta_1/\tau_\omega).dp/dx]$ is the ratio of the pressure gradient term to the drag force term in the momentum integral equation:

$$\frac{d}{dx}(\rho_G u_G^2 \delta_2) = \tau_\omega + \delta_1 . dp/dx$$

It/

It is evident from Fig. 14 that the three pressure gradients can be described either as mild or moderate and it should be stressed here that with the present apparatus, it is not possible to obtain significantly stronger pressure gradients.

It has already been stated in Section 3.3 that the boundary layers did not become fully turbulent until port 4 had been reached. The pressure gradient parameter $[(\nu_\omega/u_\tau^3 . \rho_\omega).\ dp/dx]$, plotted in Fig. 13, is a measure of the tendency for the flow to relaminarise; although not strong enough to relaminarise a fully turbulent boundary layer in the measured region, it may be expected that the pressure gradient in the section upstream of port 1 was sufficiently strong to overcome the effect of the boundary layer trip. The profiles at ports 1 and 2 bear a strong resemblance to those presented by Michel et al.[2] in a strong favourable pressure gradient.

The distribution of skin friction obtained from surface tube measurements is shown on Fig. 4a along with Spalding-Chi[3] values (for zero pressure gradient flow at the respective Mach numbers and R_2). The coefficients of skin friction show a maximum deviation of 3% from a smooth line with the exception of the one at port 6. The discrepancy of the value at port 6 may be due to a local variation in pressure gradient or a reading error; the latter possibility is supported by the inspection of the appropriate velocity profiles in log-linear co-ordinates. The values of the measured skin friction are lower than the Spalding-Chi values up to port 6 and are about equal from ports 7 to 9. This is somewhat in disagreement with what one expects in a favourable pressure gradient. But, on taking into account the facts that (a) the boundary layer was not fully turbulent in the initial region, (b) the pressure gradient was mild in the downstream section, and (c) the difference of up to 2% in the calibration of the surface tube, the results are considered to be satisfactory.

The experimental values of momentum thickness shown on Fig. 5 are in good agreement with those evaluated from the momentum integral equation using the experimental values of skin friction. The deviation is less than 4% in the favourable pressure gradient region (i.e. up to port 9). Downstream of port 9 the deviation increases to around 10%; this increase may have been caused by the reversal of the pressure gradient, by local irregularities in the pressure distribution, by weak shocks originating from the join in the roof, or by the convergence effect due to the growth of the boundary layer on the side walls; the first three effects cannot be estimated while the fourth can, and in the present case accounts for not more than 2% of the discrepancy in the section downstream of port 9.

5.2 The adverse pressure gradient

The velocity profiles shown in Fig. 8 do not indicate a log law region prior to port 4. In addition the profiles tend to deviate from the log law between ports 8 and 10 where part of the deviation is caused by the adverse pressure gradient as seen from Fig. 11; at port 11 the pressure gradient becomes favourable and the profile returns to log law.

The experimental values of skin friction coefficient shown on Fig. 4b lie on a smooth curve with a deviation of up to 3% with the exception of ports 10 and 12, where the skin friction coefficient is higher than that given by the smooth curve by approximately 7%. The values of experimental

skin friction coefficient are always less than the Spalding-Chi values and in the adverse pressure gradient region by an average of 10%. This is in accordance with the expected trend.

The experimental values of momentum thickness shown on Fig. 5 have a maximum deviation of 4% up to port 10, from the corresponding values calculated from the momentum integral equation and the measured values of skin friction. At ports 11 and 12 the deviation is approximately 8%.

5.3 The second favourable pressure gradient

In this case all the profiles indicate a logarithmic region, the long strip of carborundum having successfully tripped the boundary layer.

The values of skin friction coefficient shown on Fig. 4c indicate a maximum deviation of 4% from a smooth curve. The measured values of skin friction are higher than the Spalding-Chi values up to port 4 where the pressure gradient is strongest and tends to less than the Spalding-Chi values by an average of 3% in the region downstream. This is similar to what was observed in the downstream region of the first favourable pressure gradient.

Measured values of momentum thickness show less than 3% deviation from the corresponding momentum integral equation values. In this case no measurements were made downstream of port 10.

5.4 The zero pressure gradient results of Ref. 1

The values of momentum thickness presented in Ref. 1 have been recalculated using the procedure discussed in Section 4. In addition, a small error in the half height of the total pressure probe has been corrected. Figs. 10a and 10b show the recalculated velocity profiles and Fig. 6 the corrected momentum thickness.

5.5 The law of the wall

The velocity profiles presented in Figs. 7 to 10 are in compressible law of the wall co-ordinates (u^+, y^+). The compressible law of the wall used in this report is based on mixing length assumptions similar to those used in incompressible flow, i.e.:

$$\tau \ (= \tau_\omega) = K^2 y^2 \left(\frac{du}{dy}\right)^2$$

and is given by:

$$\frac{u_G}{u_\tau}\left\{\frac{1}{\alpha}\sin^{-1}\left(\alpha\frac{u}{u_G}\right)\right\} = \frac{1}{K}\log_e\left(\frac{u_\tau y}{\nu_\omega}\right) + \text{const.}$$

where,

$$\alpha^2 \text{ is equal to } \left[\frac{\gamma-1}{2} r M_G^2 \Big/ \left(1 + \frac{\gamma-1}{2} r M_G^2\right)\right]$$

Defining/

Defining u^+ as $\left[\frac{u_G}{u_\tau}\left\{\frac{1}{\alpha}\sin^{-1}\left(\alpha\frac{u}{u_G}\right)\right\}\right]$ the law becomes:

$$u^+ = A \log_{10} y^+ + C .$$

A and C are taken as 5·75 and 5·0, respectively, in accordance with Ref. 8 and the recovery factor r taken as 0·9 in all relevant calculations.

Some other forms of the law of the wall have been presented in Ref. 4 and commented upon; the present form has been preferred for its simplicity and suitability for adiabatic flows (see Ref. 5). Some authors - e.g. Winter et al.[6] - however, have used the incompressible form of the law of the wall:

$$\frac{u}{u_\tau} = A \log_{10} y^+ + C ;$$

but it is evident from Fig. 11 that the difference between u/u_τ and u^+ is significant at higher values of u/u_G (and at high Mach numbers). The results presented in Figs. 7 to 9 may suggest that the incompressible form of the log law will give equally good, if not better, agreement with experimental profiles; but it must be remembered that the corresponding skin friction values are in general lower than expected and there is an uncertainty of 2% in the surface probe calibration. This accounts for part of the disagreement between the experiment and the compressible log law. The case for the compressible log law is strongly supported in Ref. 5 where a wide range of compressible flow data is analysed.

The effect of pressure gradient on log law is obtained by assuming

$$\tau = \tau_\omega + y.\frac{\partial \tau}{\partial y} = \tau_\omega + 0{\cdot}5\frac{dp}{dx}$$

and, is given by:

$$u^+ = A \log_{10} y^+ + \frac{1}{4K\tau_\omega}\frac{dp}{dx}.y + C = A\left(\log_{10} y^+ + \frac{1}{1{\cdot}6A.\tau_\omega}.\frac{dp}{dx}\right) + C ;$$

and tends to decrease the discrepancy between the experiment and the log law for adverse pressure gradients while increasing it for favourable pressure gradients at higher values of y^+ (greater than 100). The use of a slightly larger value of C (say 5·5) will yield improved agreement between the experiments and the law of the wall. This in turn implies that the use of a form similar to that used by Rotta[7], also based on mixing length, (where the constants A and C are given by

$$A = 5{\cdot}75.(1{\cdot}0 - 0{\cdot}2\,M_\tau)^{\frac{1}{2}}$$

and/.

and

$$C = (1{\cdot}0 - 0{\cdot}2\, M_T)^{\frac{1}{2}} . (5{\cdot}2 + 5\, M_T)$$

where

$$M_T^2 = \tau_\omega / \gamma p$$

is desirable. The choice of M_T as the variable defining A and C was based on the analysis of a small range of high Mach number data and it may be preferable to replace M_T as the independent variable, as suggested by Bradshaw[8], and suitably redefine A and C.

5.6 The floating element balance measurements

Floating element balance measurements in pressure gradients are presented in Fig. 15 in the form of an error plot (assuming surface probe results to be correct); the results of Ref. 1 are also included. The Figure shows a lack of correlation which may be due to the experimental uncertainty in the surface probe and the floating element balance measurements as well as the occurrence of a few feeble measurements among the floating element balance results. Brown and Joubert[9] report the occurrence of secondary forces of up to 15% of the local shear stress with "some" correlation with pressure gradient in flows where the direct effect of the pressure gradient is only 3% of the local shear stress. This condition corresponds to $[dp/dx).\ D/\tau_\omega]$ approximately equal to 0·001 for the floating element balance used in the present work; and it is possible to use the floating element balance to an accuracy of the order 5% in mild pressure gradients $(dp/dx.\ D/\tau_\omega < 0{\cdot}002)$.

6. Conclusions

1. Measurements of velocity profiles and skin friction in three pressure gradients are presented in the present report and form suitable test data for the study of prediction methods. One of the favourable and the adverse pressure gradient data cover a wide Mach number range but the other favourable pressure gradient covers a smaller Mach number range.

2. The data of Ref. 1 are found to be of better precision than apparent in Ref. 1, but the conclusions of Ref. 1 are still valid.

3. The floating element balance cannot be reliably used in strong pressure gradients but is usable in mild pressure gradients to an accuracy of 5%.

Acknowledgements

The author wishes to thank Dr. J. H. Whitelaw and Mr. P. Bradshaw for their useful advice and assistance in producing the present report. The author also acknowledges the co-operation of the N.P.L. Aerodynamics Division Workshop staff, especially that of Mr. G. Hellens, who made the reported modifications to the wind tunnel. Further, acknowledgement is made to the Ministry of Technology who supported this work.

References/

References

No.	Author(s)	Title, etc.
1	B. Edwards and S. Sivasegaram	An experimental investigation of Mach 2·2, turbulent boundary layers in nominally zero pressure gradients. Dept. of Mech. Eng., Imperial College, London. BL/TN/3. 1968.
2	R. Michel, C. Quémard and M. P. Elena	Distributions de vitesses des couches limites turbulentes en écoulement compressible, uniforme ou accéléré. La Recherche Aérospatiale, No. 128, p. 33. Jan.-Feb. 1969.
3	D. B. Spalding and S. W. Chi	The drag of a compressible turbulent boundary layer on a smooth flat plate with and without heat transfer. J. Fluid Mechanics, Vol. 18, Pt 1, p. 117. January 1964.
4	S. Sivasegaram	A review of the literature pertaining to experimental investigation of the two-dimensional, compressible, turbulent, wall boundary layers. Dept. of Mech. Eng., Imperial College, London. TWF/TN/44. 1968.
5	H. E. Hügel	Velocity profiles in turbulent compressible flow. D.I.C. Thesis, Imperial College, London. 1963.
6	J. C. Rotta	Turbulent boundary layers with heat transfer in compressible flow. AGARD Report 281. 1960.
7	K. G. Winter, K. G. Smith and L. Gaudet	Measurement of turbulent skin friction at high Reynolds numbers and Mach numbers of 0·2 and 2·2. Unpublished Ministry of Technology report.
8	P. Bradshaw	Private communication.
9	K. C. Brown and P. N. Joubert	The measurement of skin friction in turbulent boundary layers with pressure gradients. J. Fluid Mechanics, Vol. 35, Pt 4, p. 737. 1969.

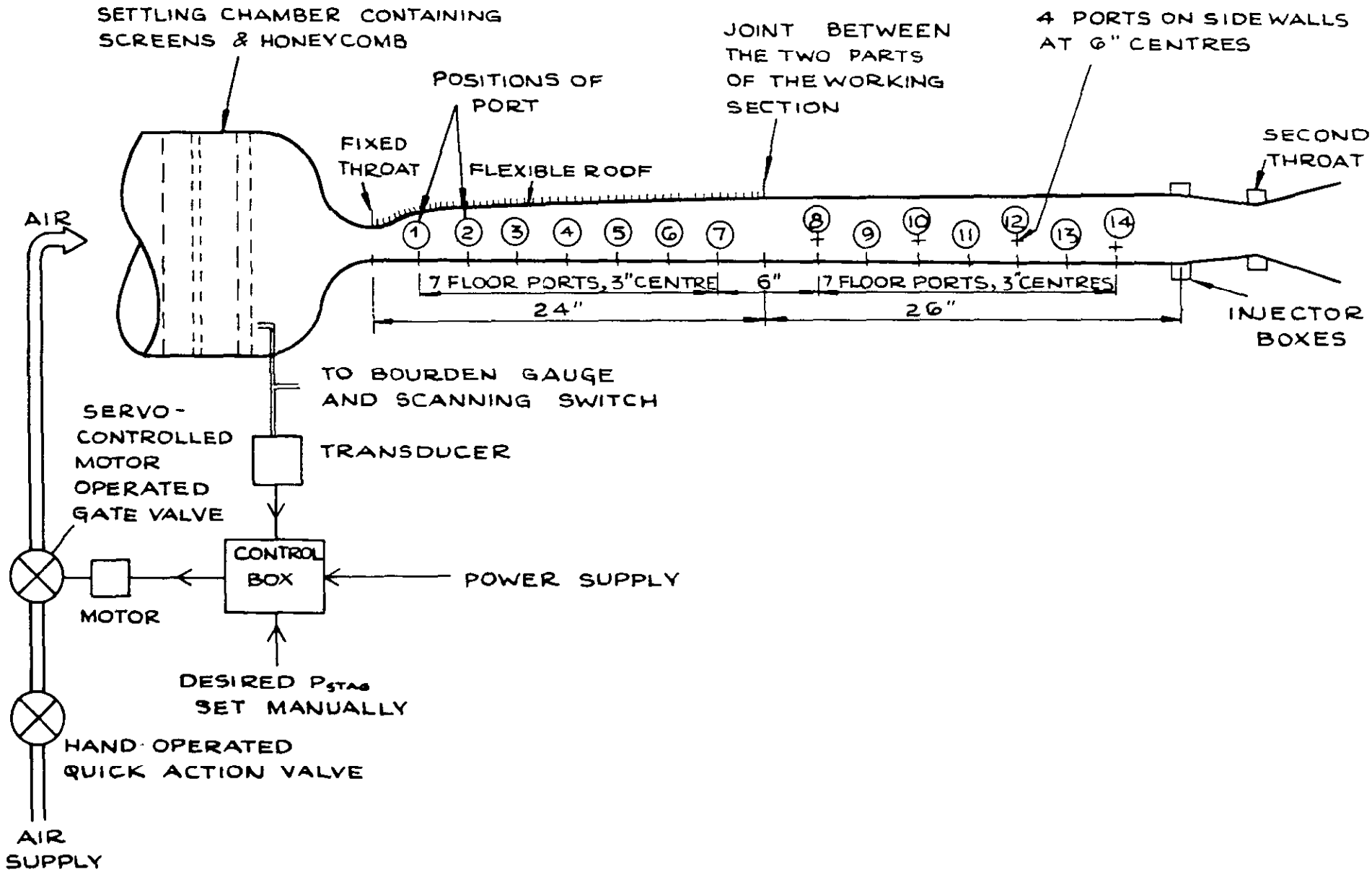

FIG 1 LAYOUT DIAGRAM OF WIND TUNNEL
(NOT TO SCALE)

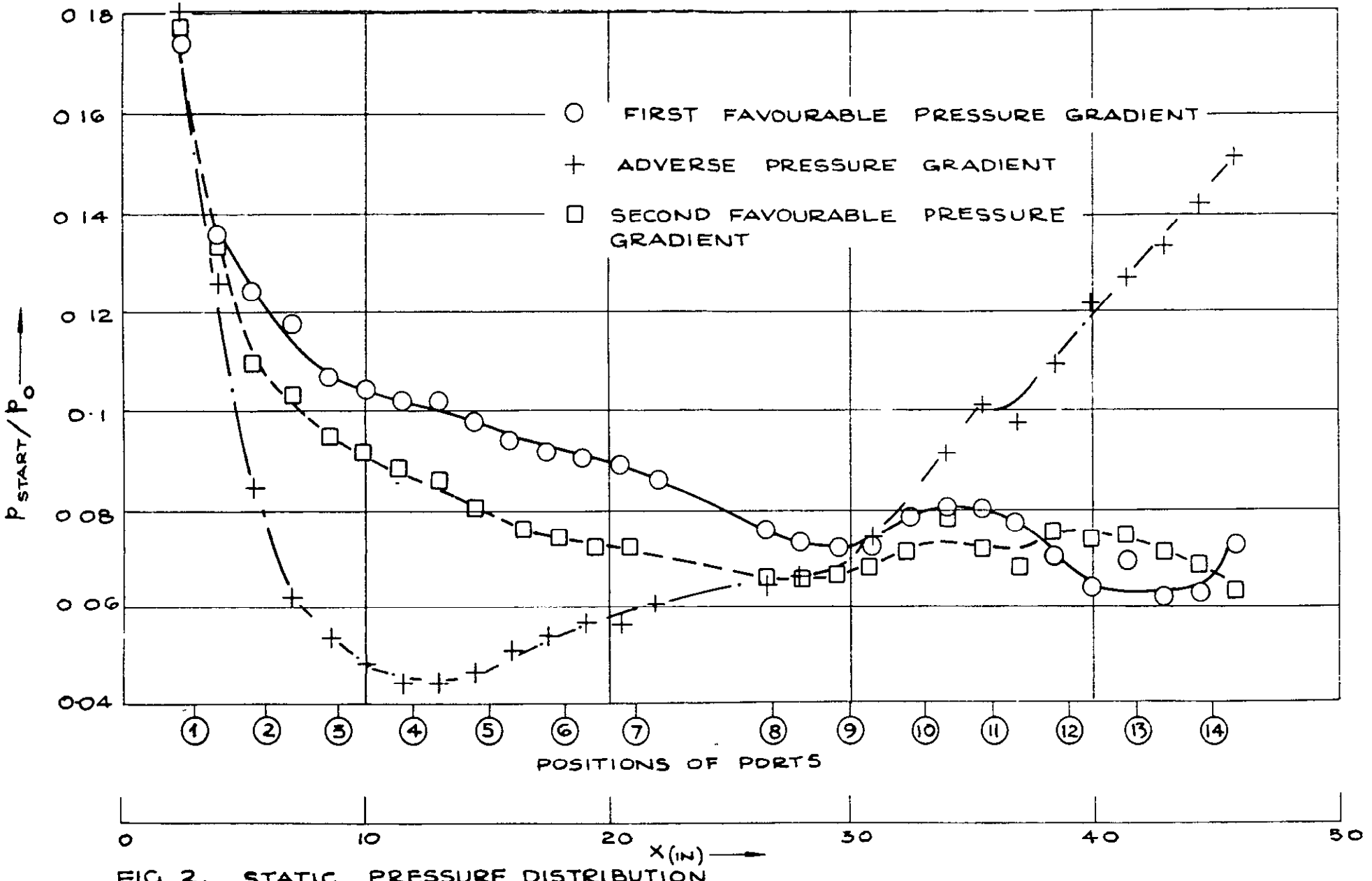

FIG 2. STATIC PRESSURE DISTRIBUTION

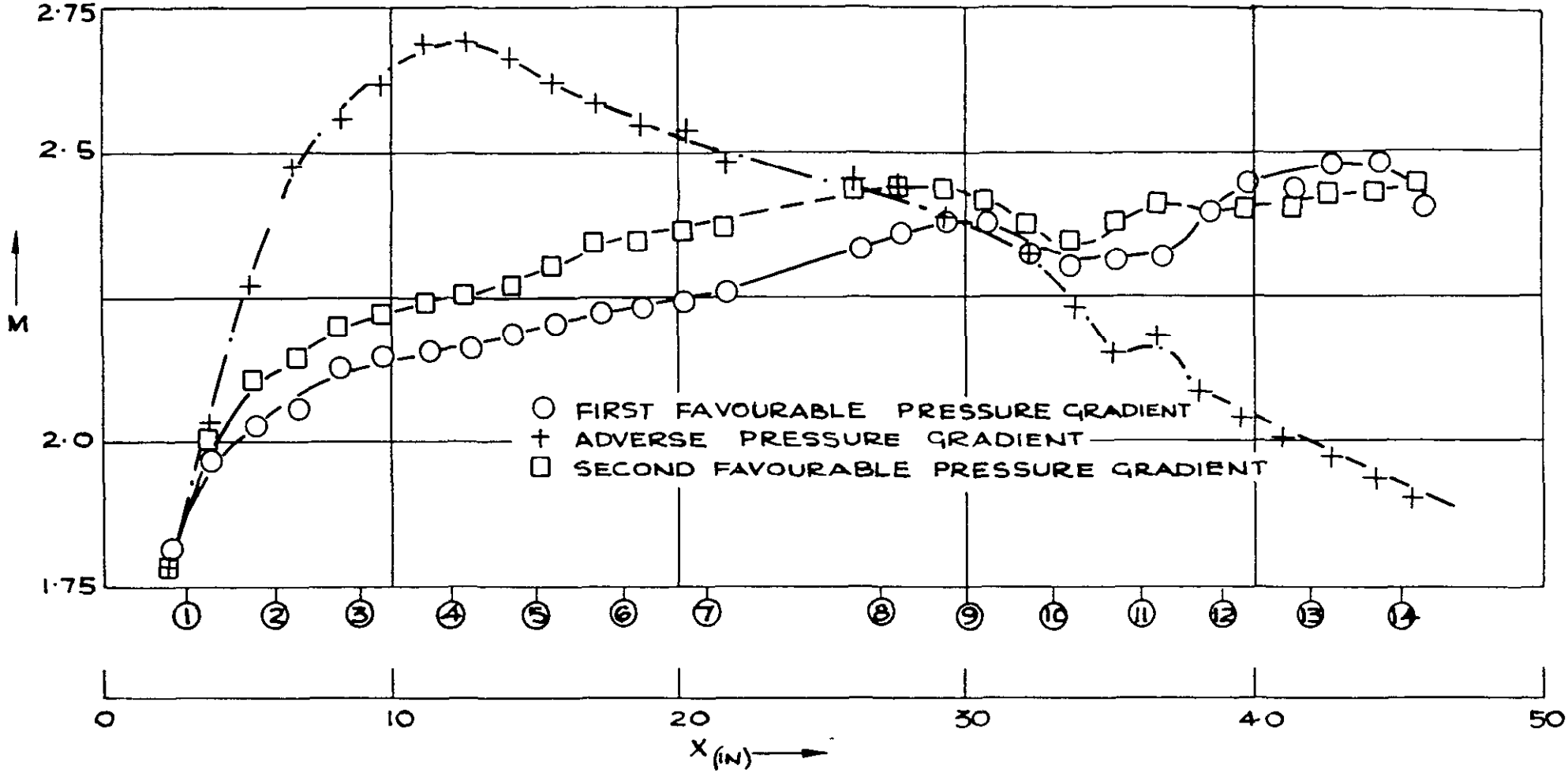

FIG. 3 : MACH NUMBER DISTRIBUTION

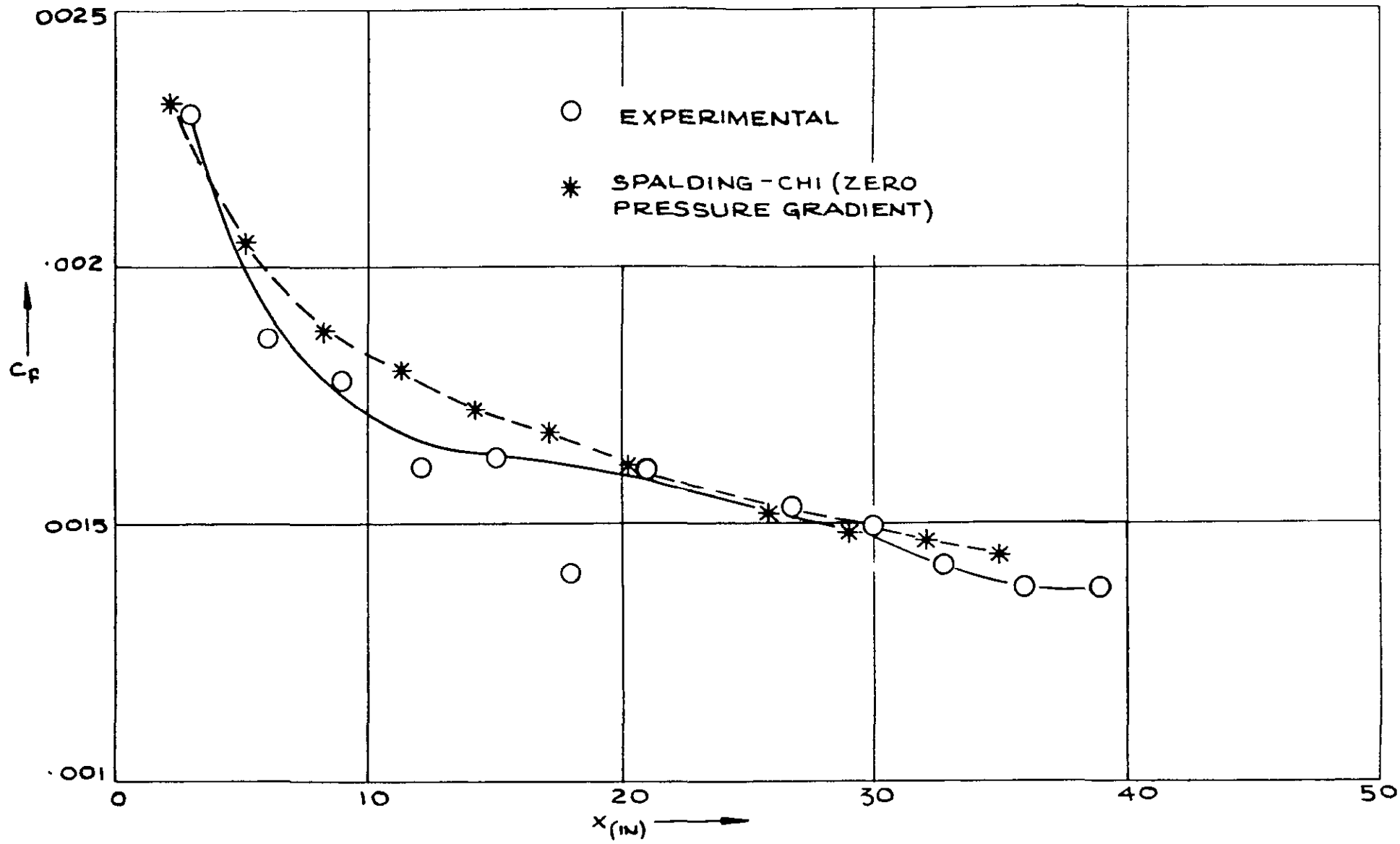

FIG 4a. SKIN FRICTION COEFFICIENT VS X (FIRST FAVOURABLE PRESSURE GRADIENT)

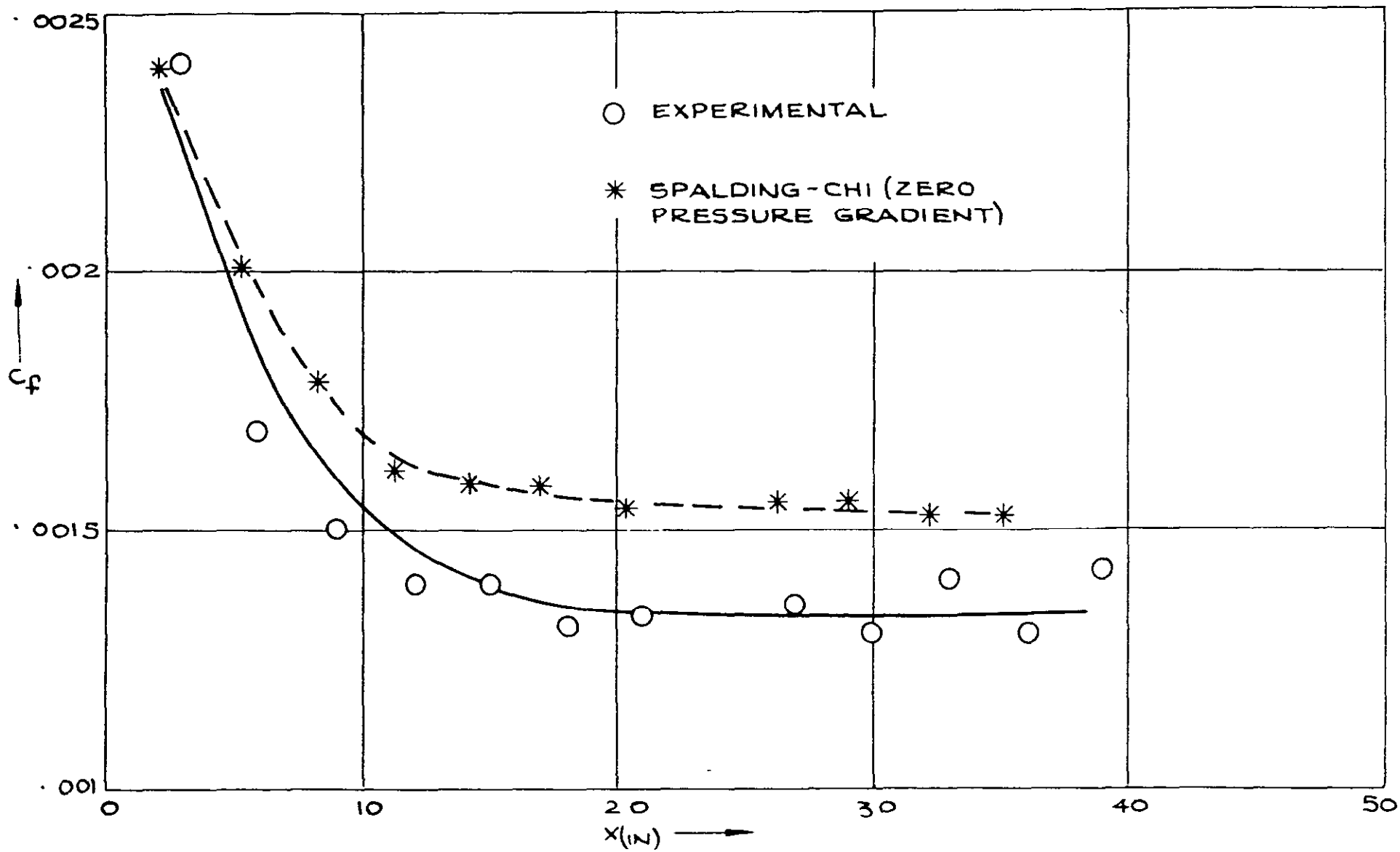

FIG 4b SKIN FRICTION COEFFICIENT VS X (ADVERSE PRESSURE GRADIENT)

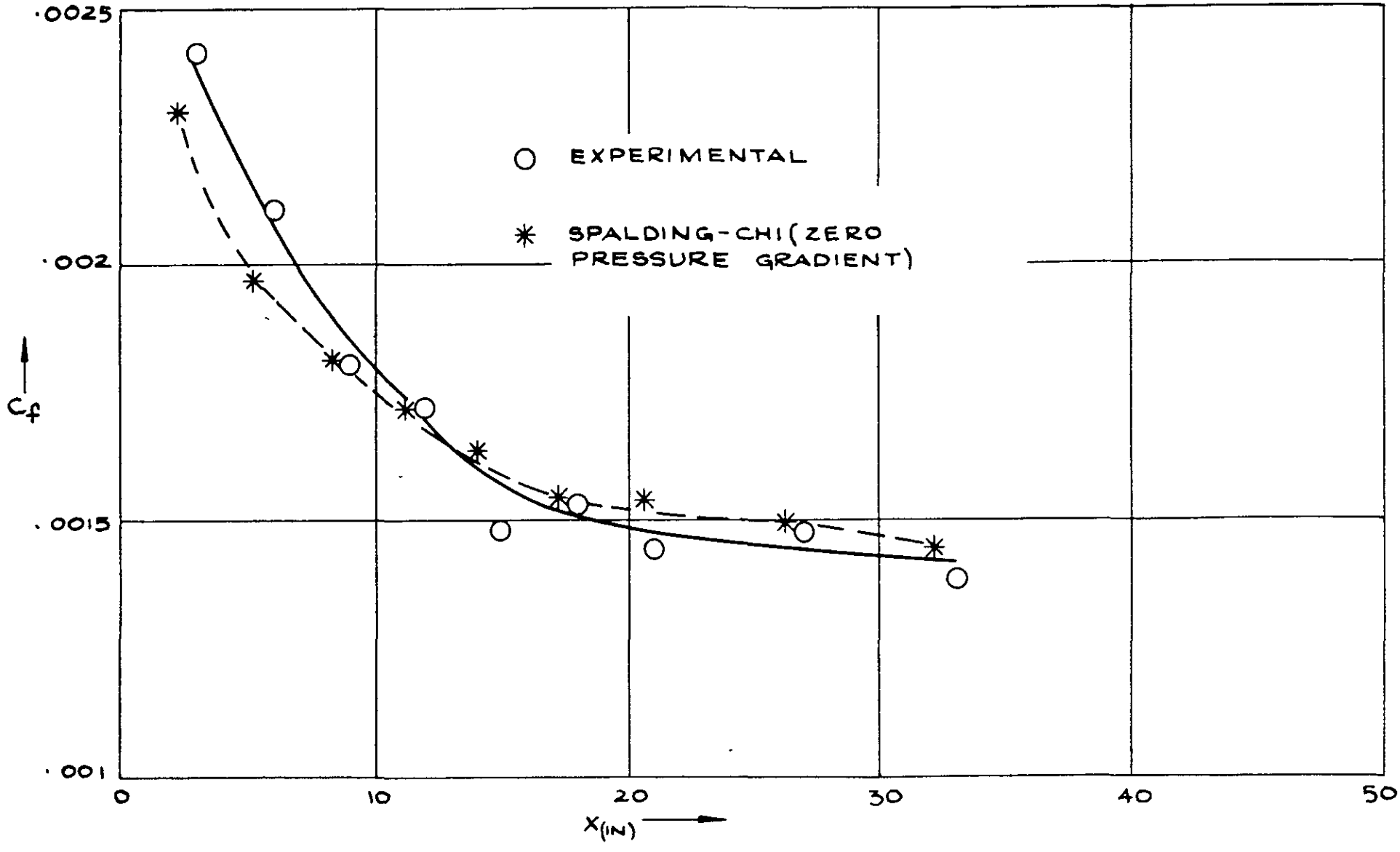

FIG 4c SKIN FRICTION COEFFICIENT VS x (SECOND FAVOURABLE PRESSURE GRADIENT)

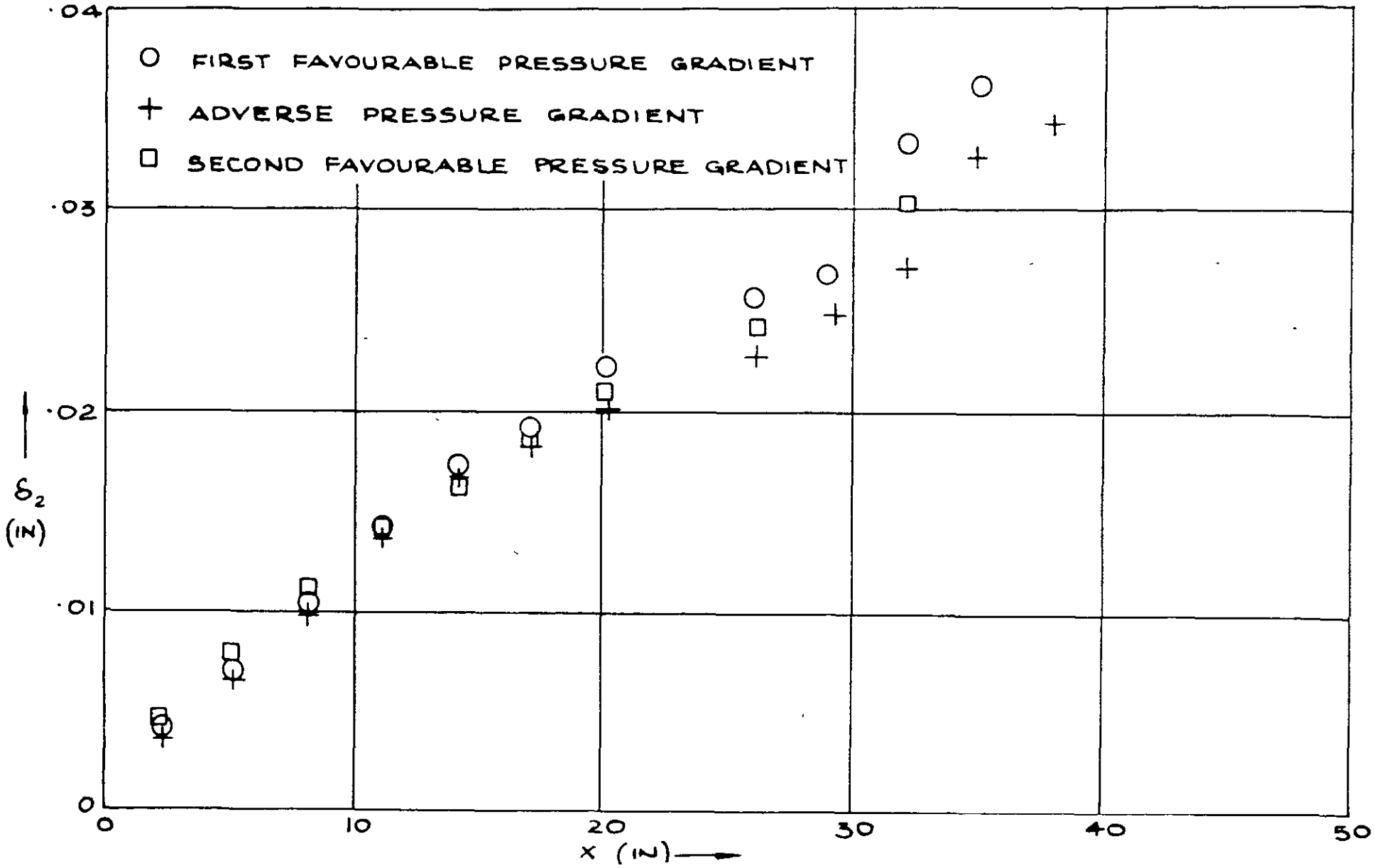

FIG 5 MOMENTUM THICKNESS VS X (PRESENT MEASUREMENTS)

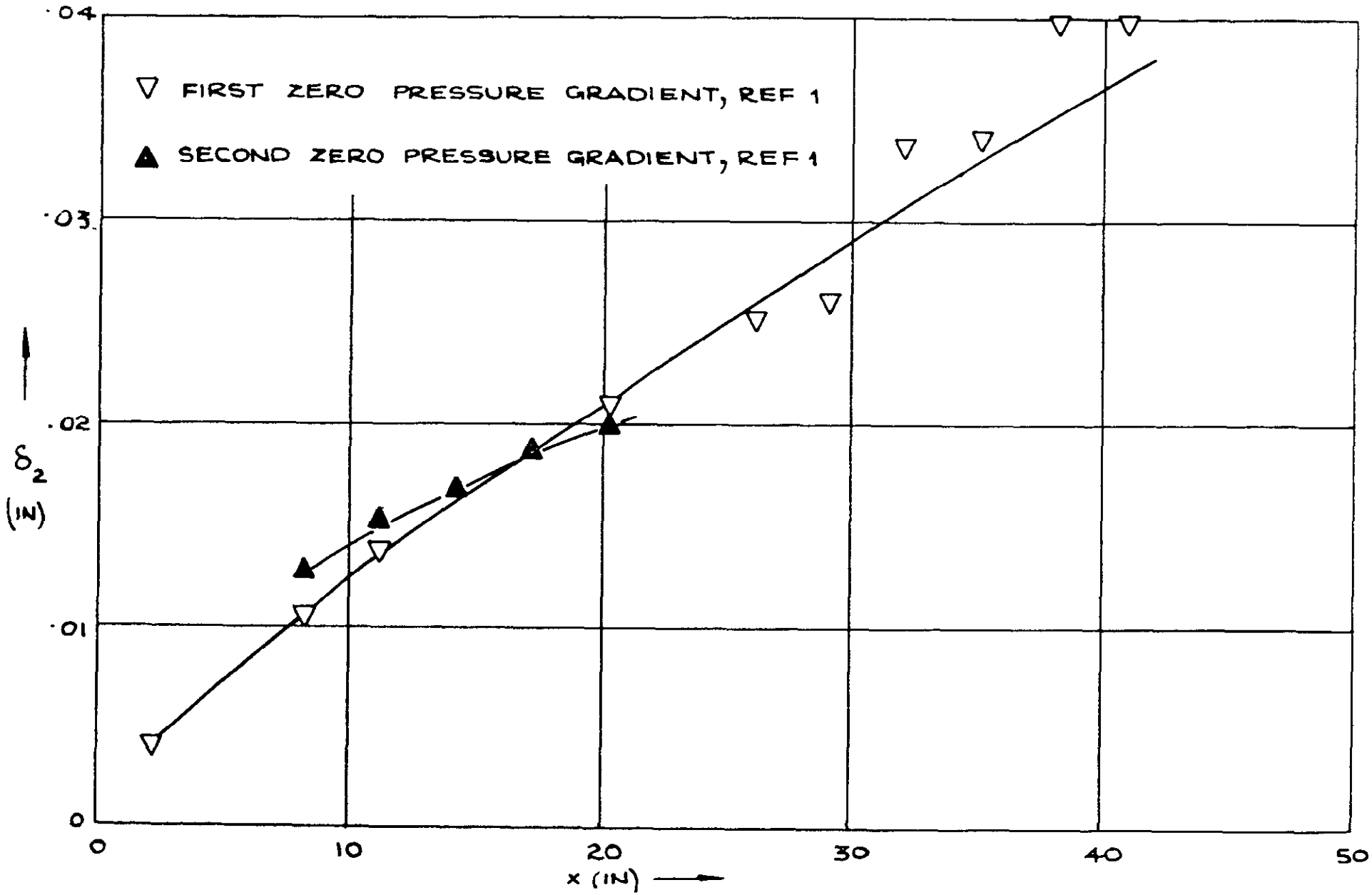

FIG. 6: MOMENTUM THICKNESS VS x (RESULTS OF REF 1, REVISED)

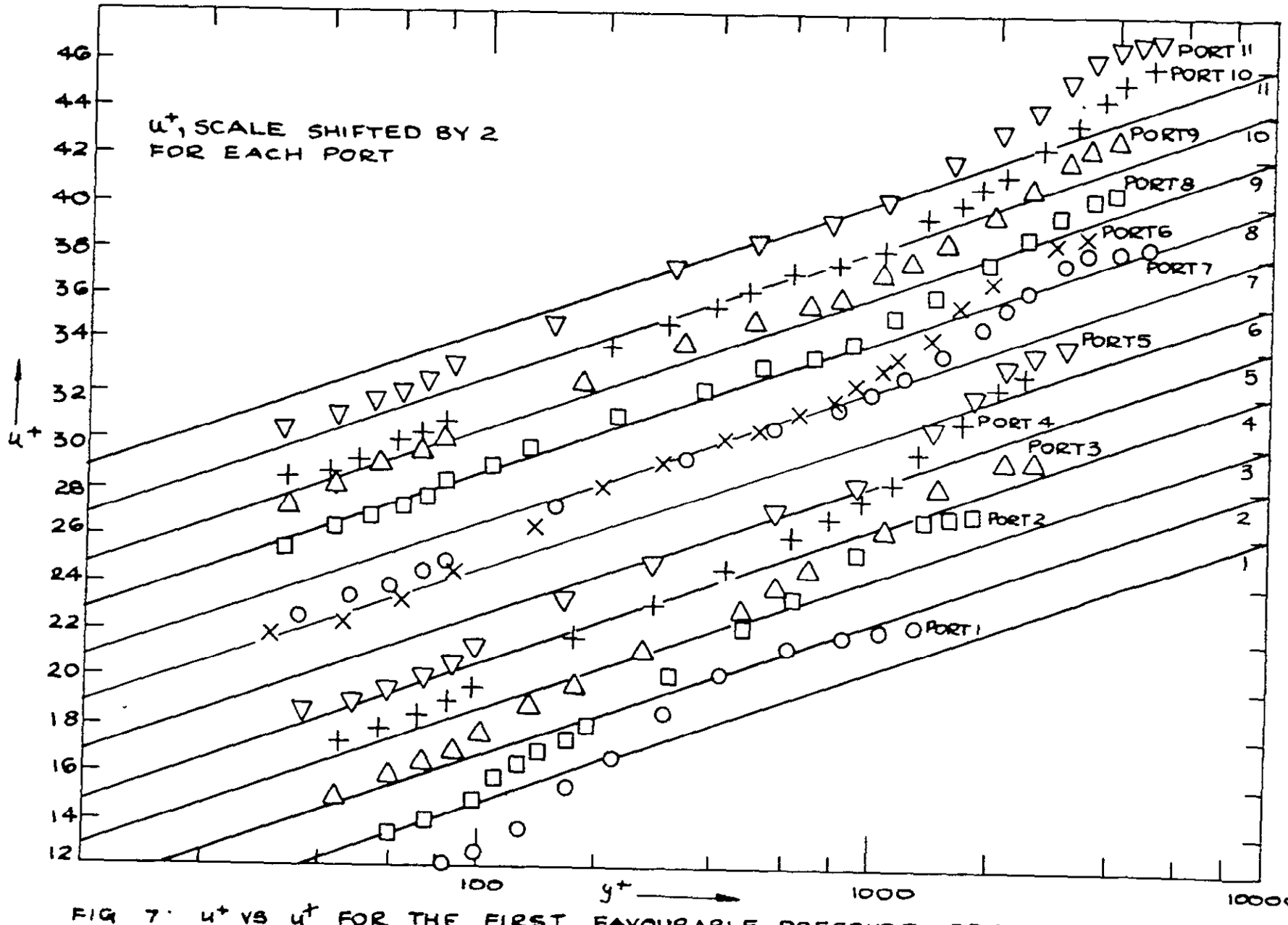

FIG 7. u^+ VS y^+ FOR THE FIRST FAVOURABLE PRESSURE GRADIENT

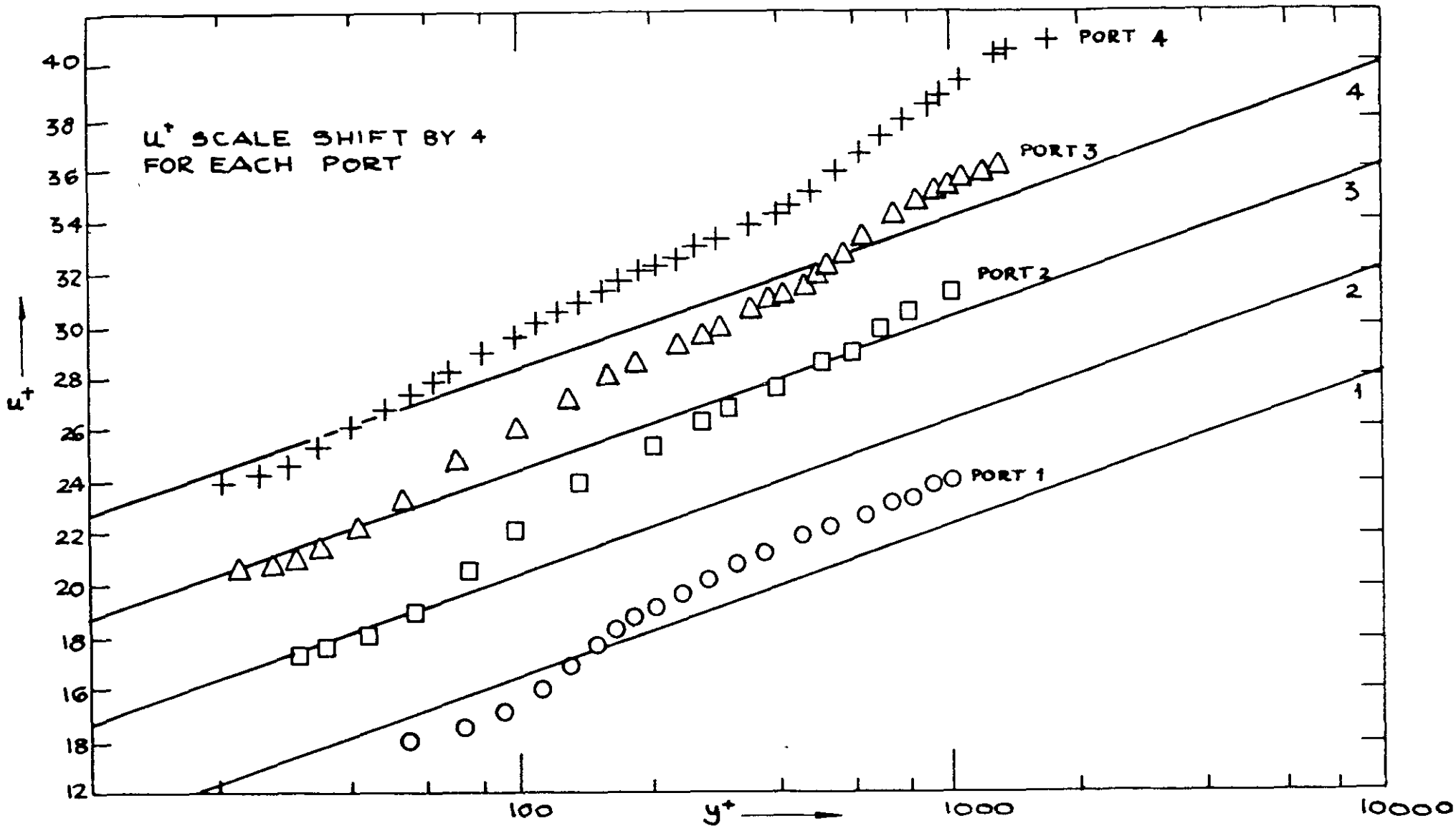

FIG 8. u^+ VS y^+ FOR THE ADVERSE PRESSURE GRADIENT

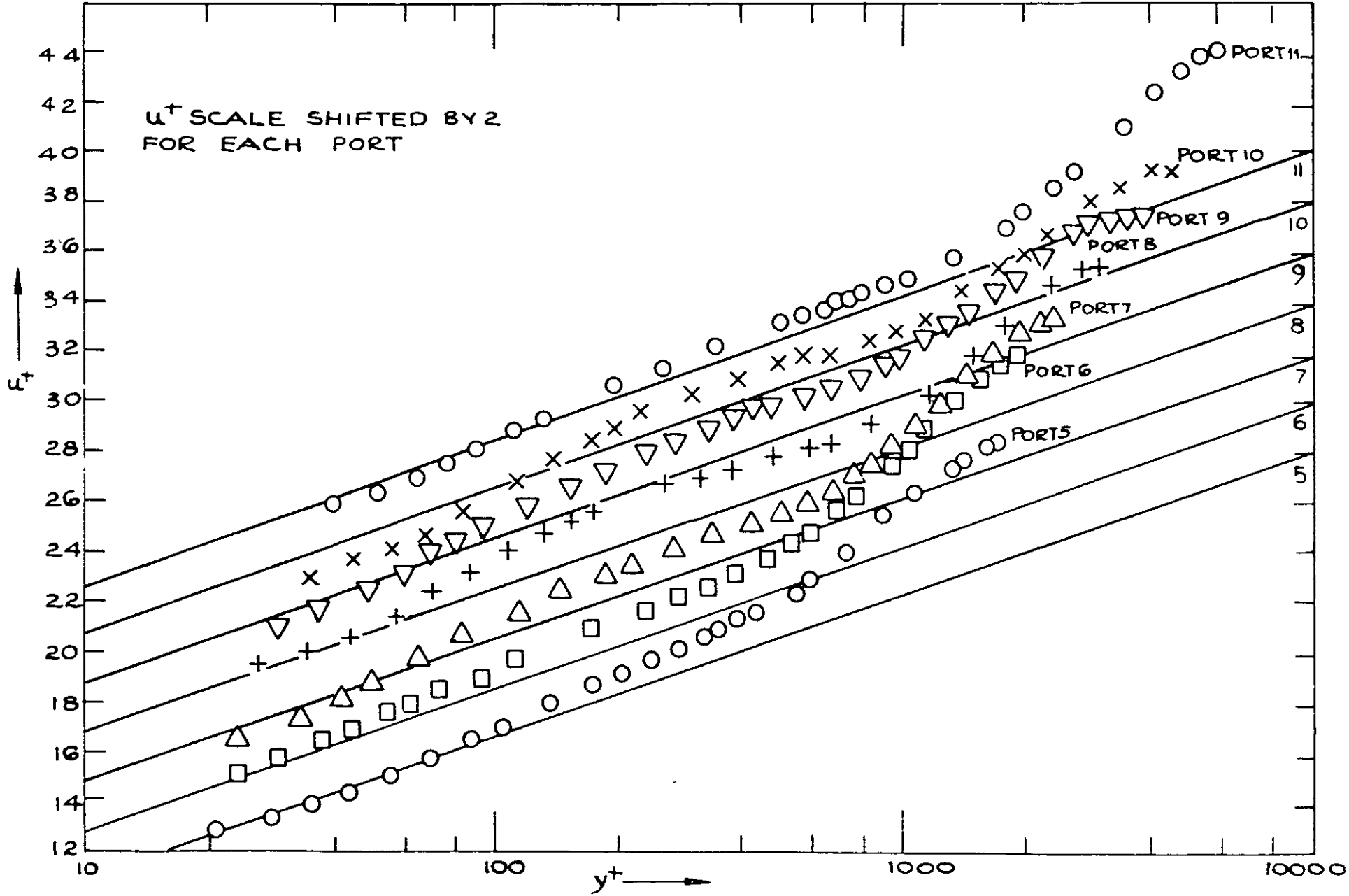

FIG 8 (CONTD.) u^+ VS y^+ FOR ADVERSE PRESSURE GRADIENT

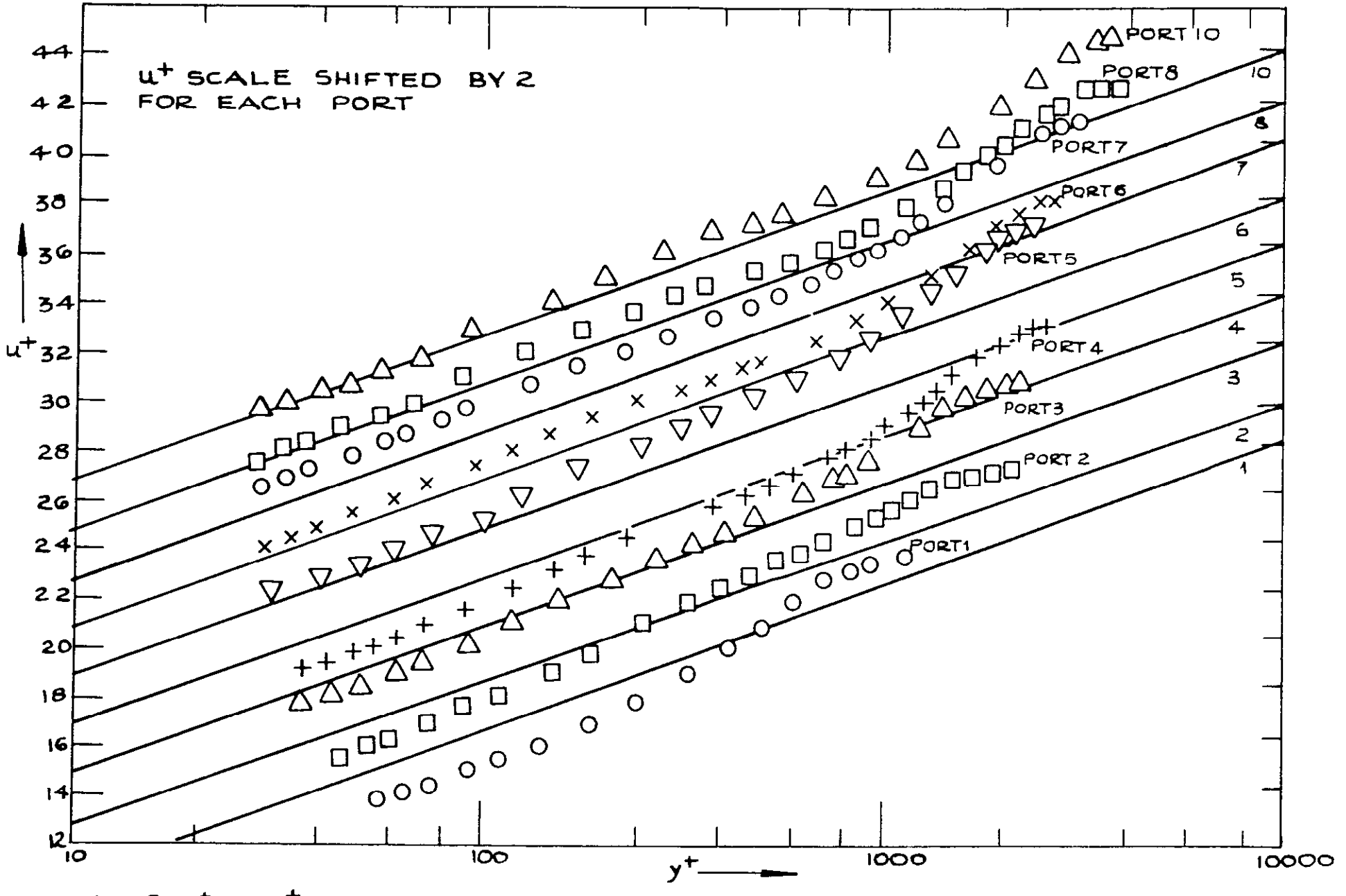

FIG.9: u^+ vs y^+ FOR SECOND FAVOURABLE PRESSURE GRADIENT

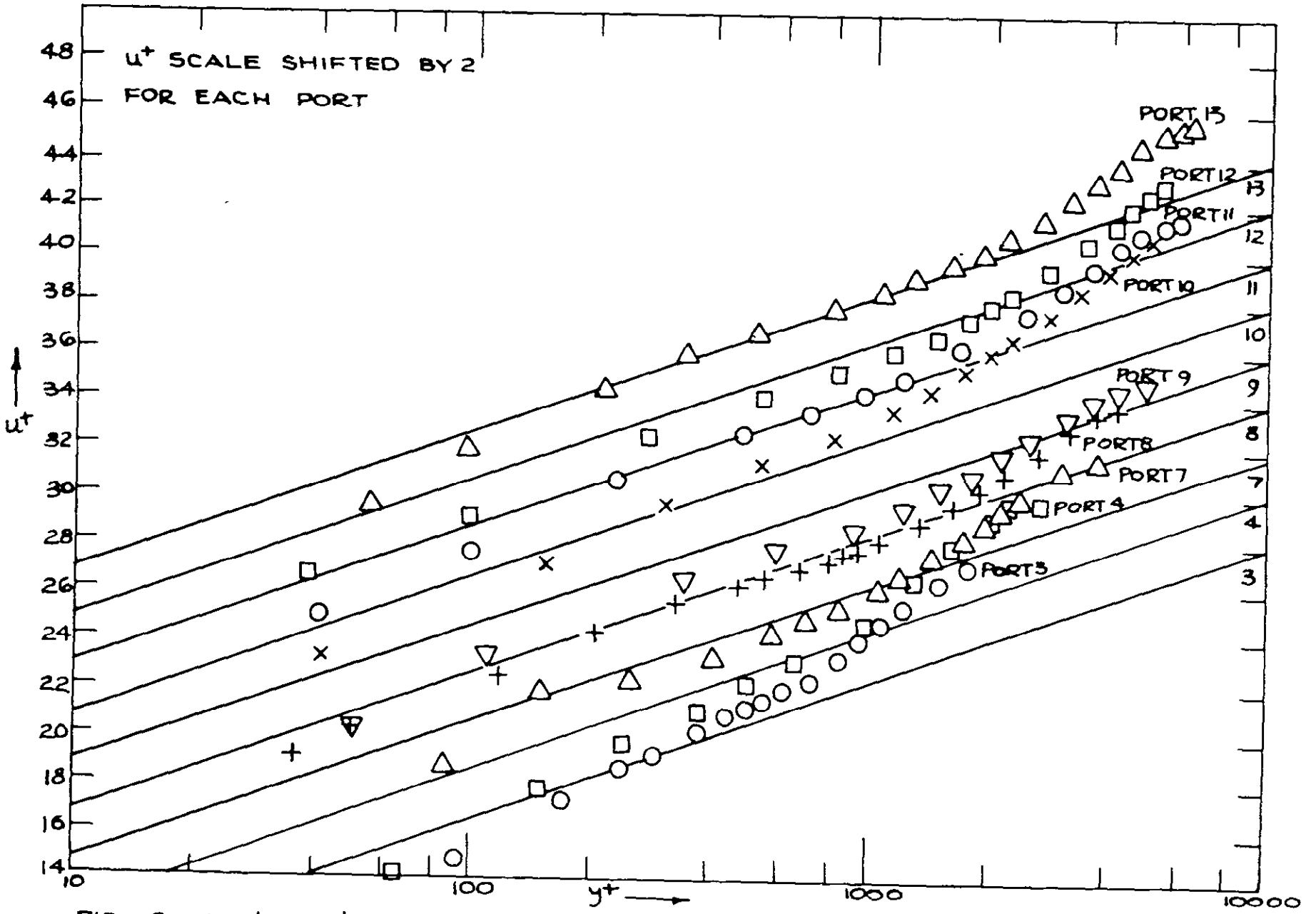

FIG 10 a : u^+ VS y^+ FOR THE FIRST ZERO PRESSURE GRADIENT, REF 1.

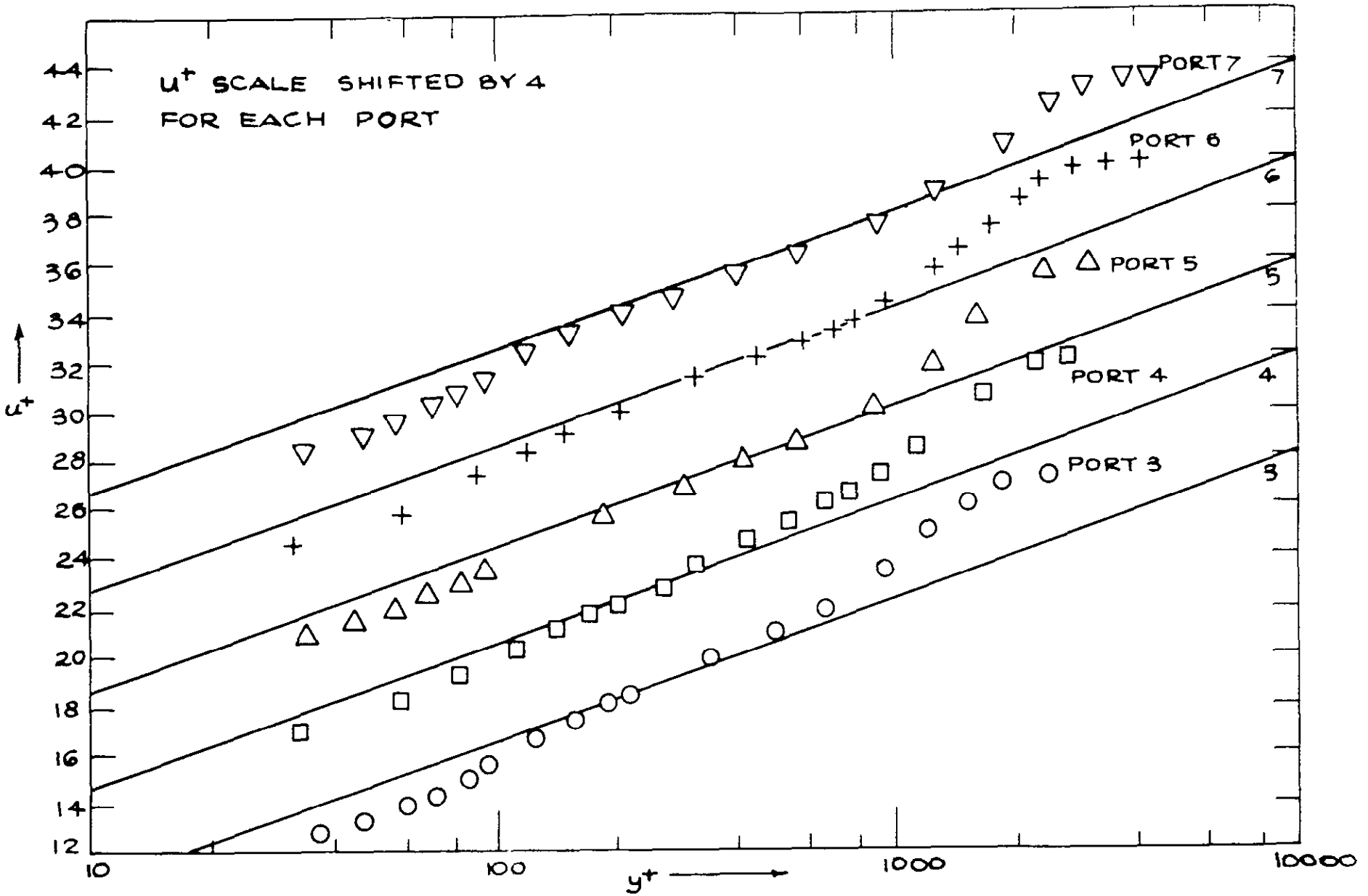

FIG 10 b' u^+ VS y^+ FOR SECOND ZERO PRESSURE GRADIENT, REF 1

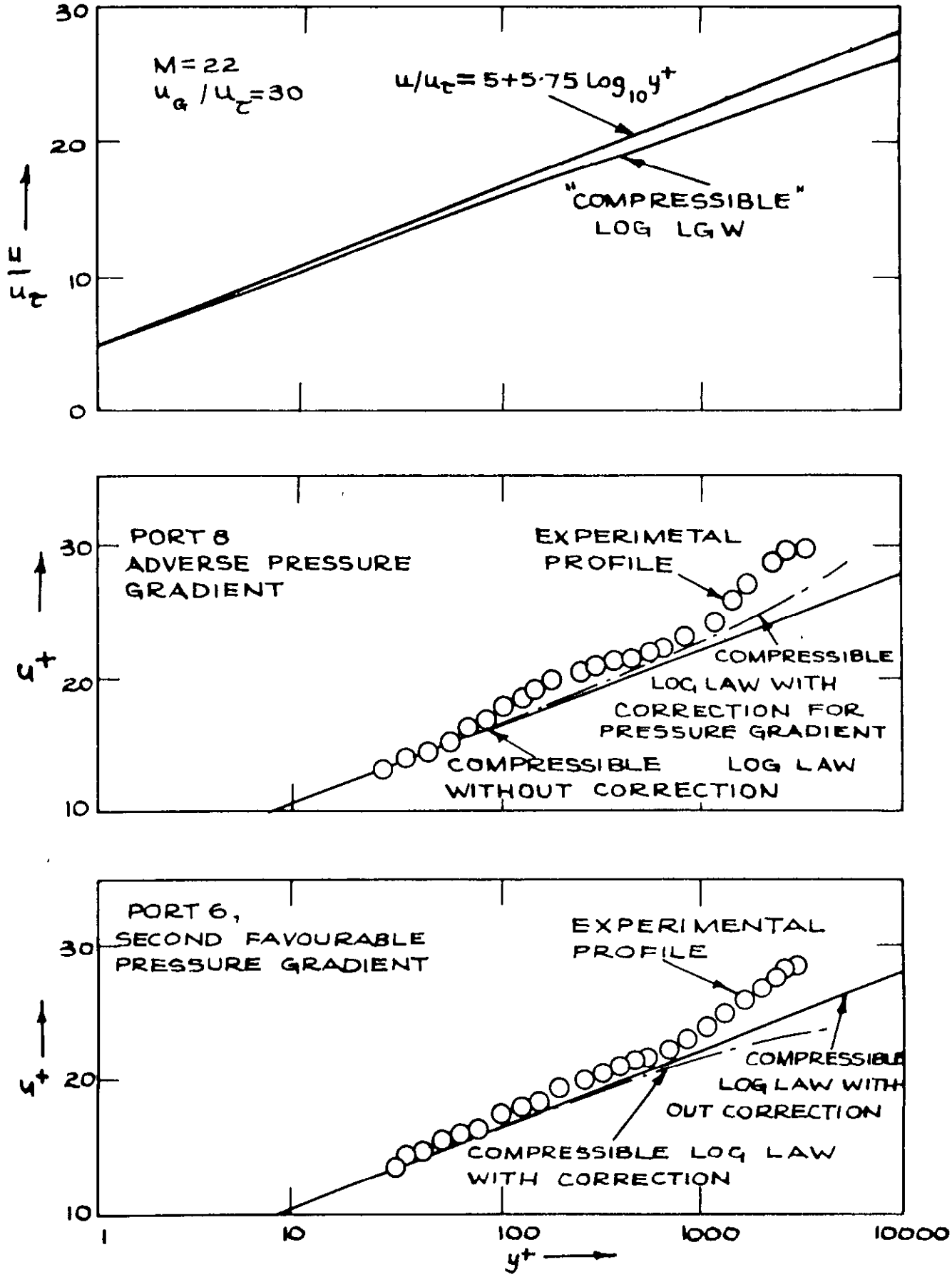

FIG 11. EFFECT OF COMPRESSIBILITY AND PRESSURE GRADIENT ON THE LAW OF THE WALL

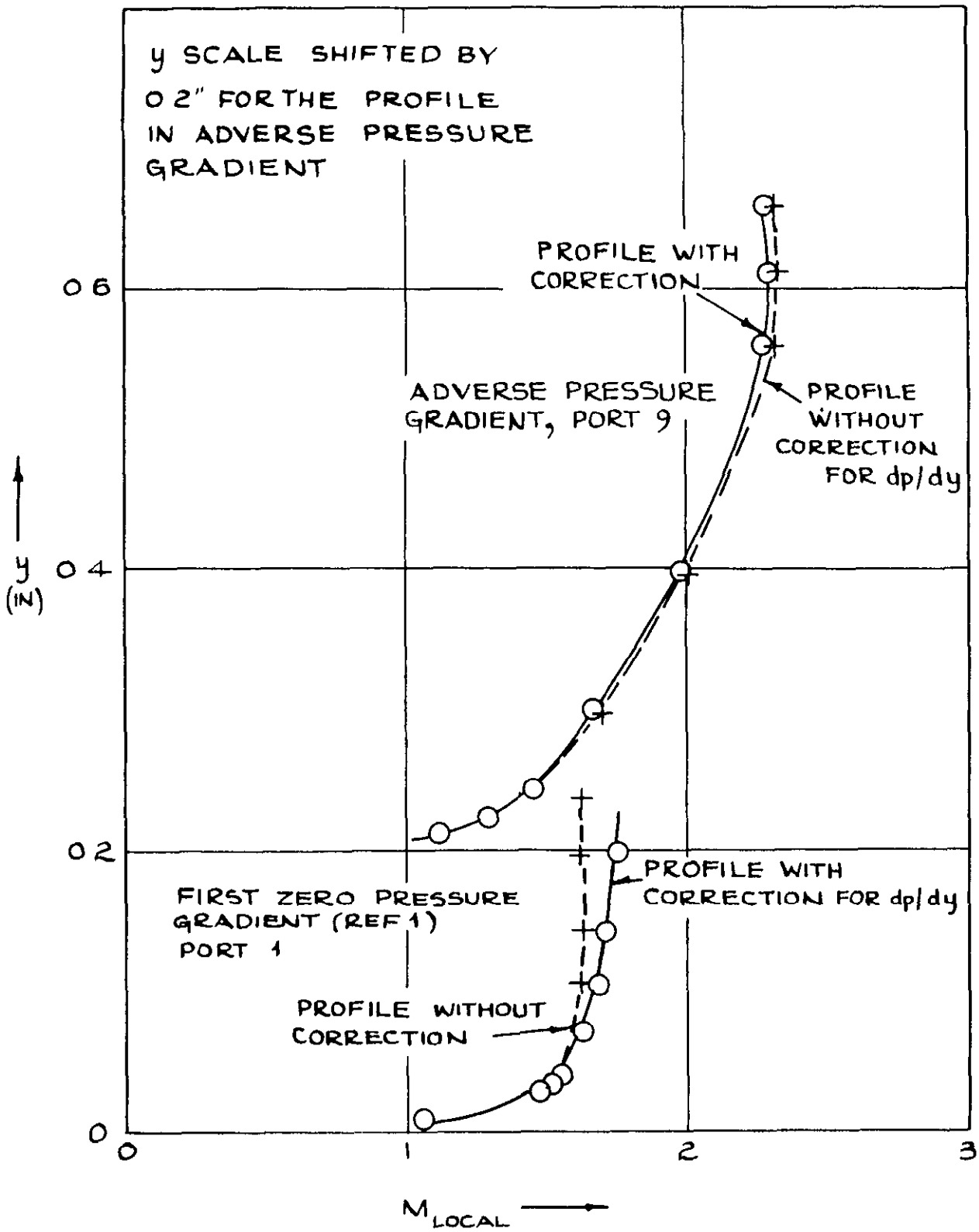

FIG 12 LOCAL MACH NUMBER PROFILES, WITH AND WITHOUT CORRECTION FOR dp/dy

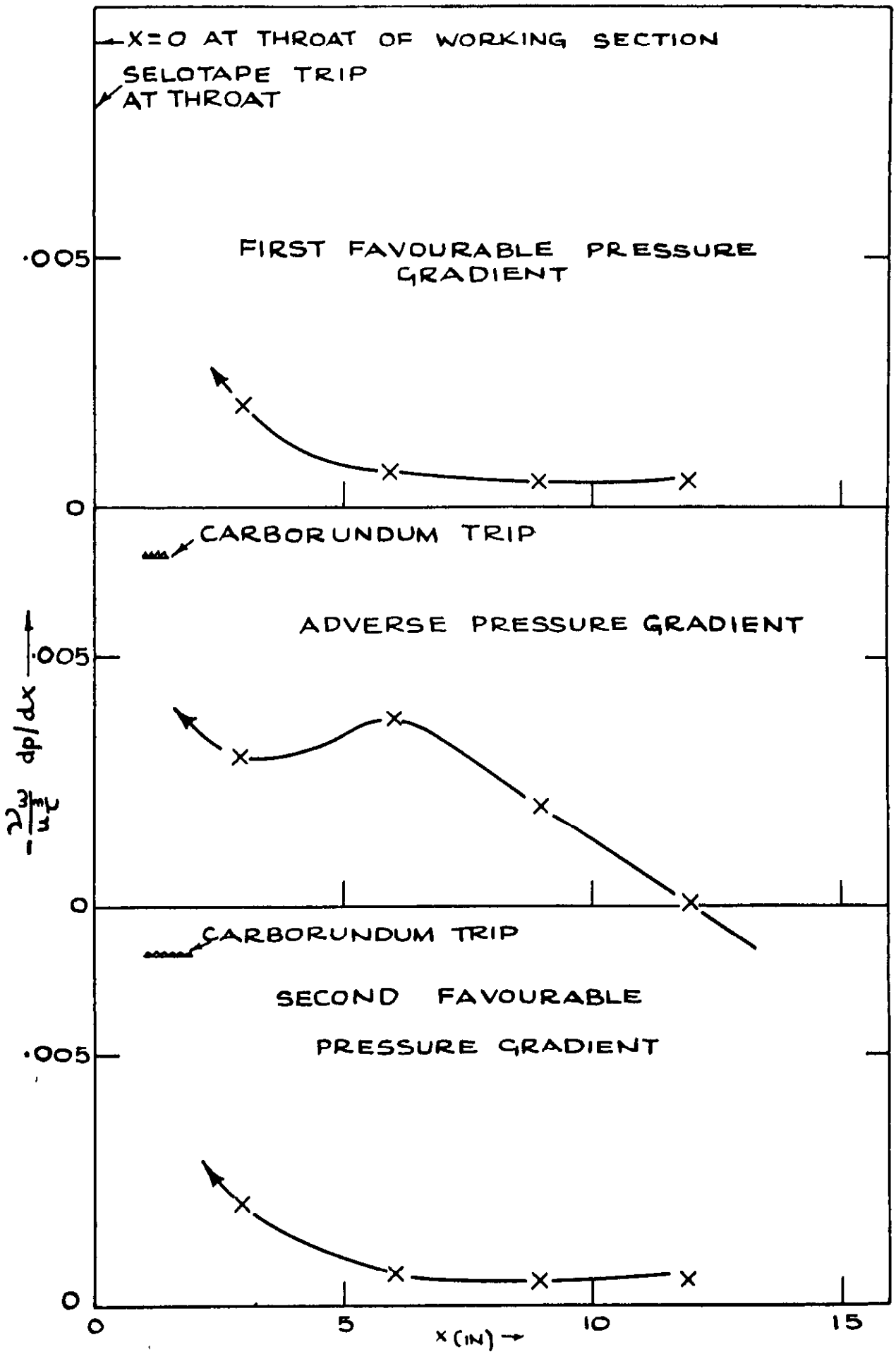

FIG. 13 $[-\nu_w / u_c^3 \tau_w \; dp/dx]$ vs x

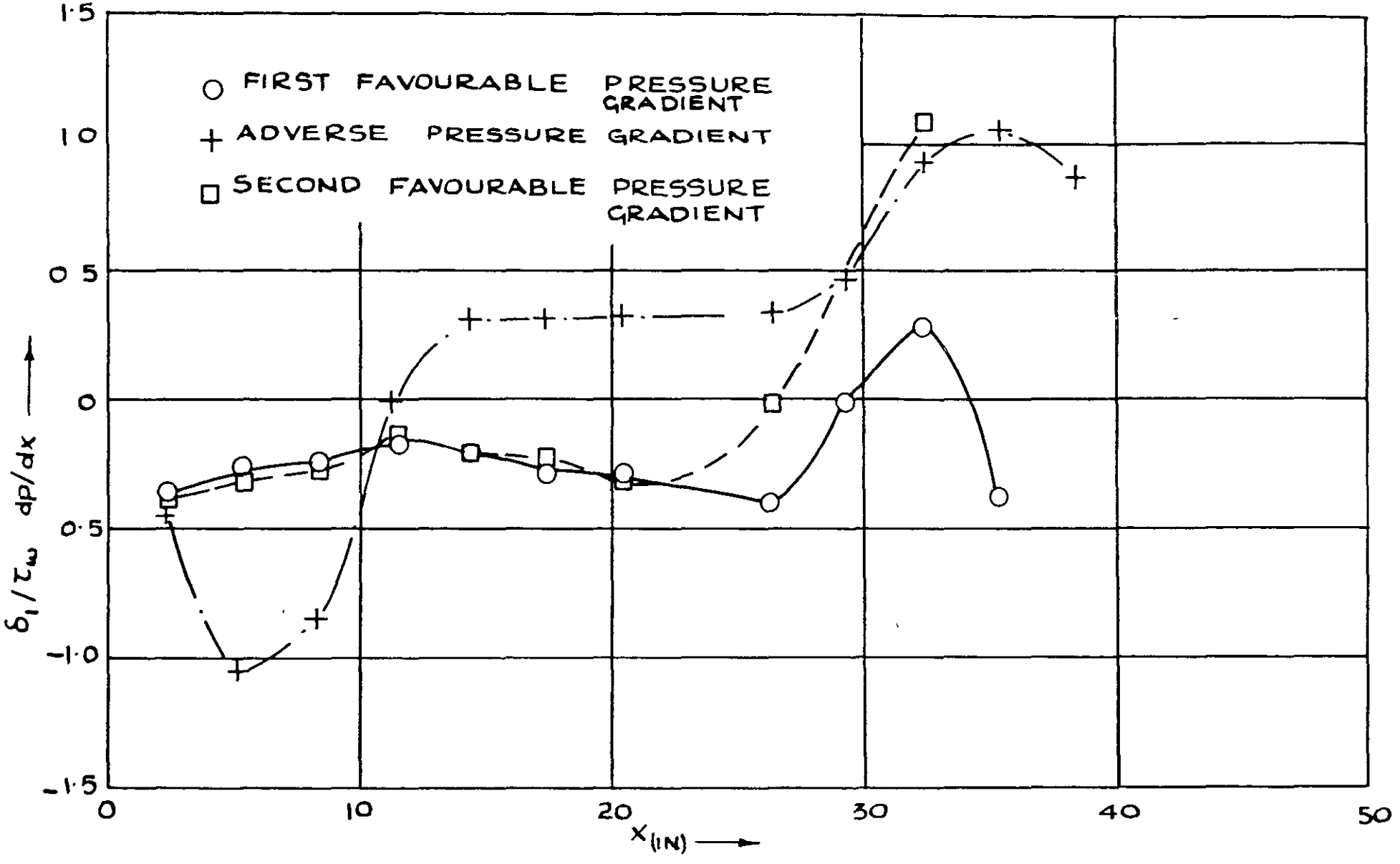

FIG 14 $\left[(\delta_1/\tau_w)\, dp/dx\right]$ VS X (BASED ON SMOOTHED CURVES FOR STATIC PRESSURE DISTRIBUTION)

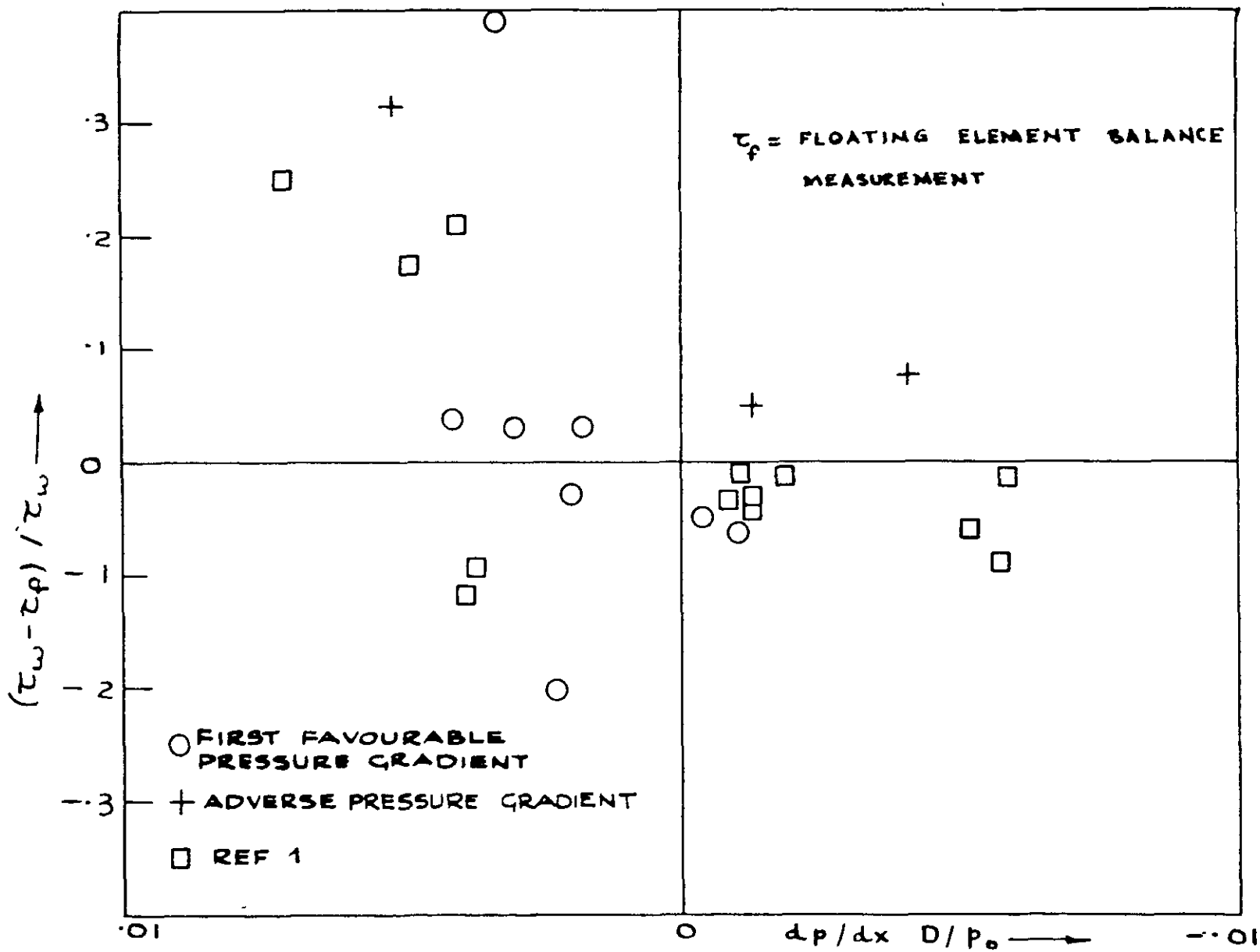

FIG. 15. ERROR PLOT FOR FLOATING ELEMENT BALANCE.

R6058/502109 K4 11/71 P

A.R.C. C.P. No.1190
July, 1969
Sivasegaram, S. Dept. of Mech. Eng., Imperial College

AN EXPERIMENTAL INVESTIGATION OF SUPERSONIC BOUNDARY-LAYER FLOWS WITH PRESSURE GRADIENTS

The report presents measurements made in the small supersonic wind tunnel at the National Physical Laboratory, Teddington. Boundary layer measurements in two favourable and one adverse pressure gradient are analysed. The report also includes a more detailed study of some zero pressure gradient measurements, made with the same apparatus and reported earlier, and a study of the performance of the floating element skin friction balance in pressure gradients.

A.R.C. C.P. No.1190
July, 1969
Sivasegaram, S. Dept. of Mech. Eng. Imperial College

AN EXPERIMENTAL INVESTIGATION OF SUPERSONIC BOUNDARY-LAYER FLOWS WITH PRESSURE GRADIENTS

The report presents measurements made in the small supersonic wind tunnel at the National Physical Laboratory, Teddington. Boundary layer measurements in two favourable and one adverse pressure gradient are analysed. The report also includes a more detailed study of some zero pressure gradient measurements, made with the same apparatus and reported earlier, and a study of the performance of the floating element skin friction balance in pressure gradients.

A.R.C. C.P. No.1190
July, 1969
Sivasegaram, S. Dept. of Mech. Eng. Imperial College

AN EXPERIMENTAL INVESTIGATION OF SUPERSONIC BOUNDARY-LAYER FLOWS WITH PRESSURE GRADIENTS

The report presents measurements made in the small supersonic wind tunnel at the National Physical Laboratory, Teddington. Boundary layer measurements in two favourable and one adverse pressure gradient are analysed. The report also includes a more detailed study of some zero pressure gradient measurements, made with the same apparatus and reported earlier, and a study of the performance of the floating element skin friction balance in pressure gradients.

DETACHABLE ABSTRACT CARDS

Produced and published by
HER MAJESTY'S STATIONERY OFFICE

To be purchased from
49 High Holborn, London WC1V 6HB
13a Castle Street, Edinburgh EH2 3AR
109 St Mary Street Cardiff CF1 1JW
Brazennose Street Manchester M60 8AS
50 Fairfax Street Bristol BS1 3DE
258 Broad Street Birmingham B1 2HE
80 Chichester Street Belfast BT1 4JY
or through booksellers

Printed in England

C.P. No. 1190

SBN 11 470458 9